International Journal of Mechanical, Industrial and Aerospace Sciences
ISSN: 2517-9950
Vol:5, No:8, 2011

Zero Dimensional Simulation of Combustion Process of a DI Diesel Engine Fuelled With Biofuels

Donepudi Jagadish, Ravi Kumar Puli and K. Madhu Murthy

***Abstract*—**A zero dimensional model has been used to investigate the combustion performance of a single cylinder direct injection diesel engine fueled by biofuels with options like supercharging and exhaust gas recirculation. The numerical simulation was performed at constant speed. The indicated pressure, temperature diagrams are plotted and compared for different fuels. The emissions of soot and nitrous oxide are computed with phenomenological models. The experimental work was also carried out with biodiesel (palm stearin methyl ester) diesel blends, ethanol diesel blends to validate simulation results with experimental results, and observed that the present model is successful in predicting the engine performance with biofuels.

***Keywords*—**Biofuels Zero Dimensional Modeling, Engine Performance, Engine Emissions

I. Introduction

COMPUTER simulation has contributed enormously towards new evaluation in the field of internal combustion engines. Mathematical tools have become very popular in recent years owing to the continuously increasing improvement in computational power. Diesel engines occupy a prominent role in the present transportation and power generation sectors. There have been many methods tried and are in use to reduce pollutant emissions from a diesel engine. The main options to reduce pollutants are the usage of biofuels and adopting some modifications to the combustion process. Diesel engine simulation models can be used to understand the combustion performance; these models can reduce the number of experiments.

Depending upon the various possible applications different types of models for diesel engine combustion process have been in use. In the order of increased complexity and increased computer system requirements these can be classified as zero dimensional models, quasi dimensional phenomenological models and Multidimensional computational fluid dynamics models [1-12].

Donepudi Jagadish is with the Mechanical Engineering Department of National Institute of Technology, Warangal-506004, Andhra Pradesh, India (e-mail:jagadish.donepudi@gmail.com, Ph: +91 870 246 2333)

Ravi Kumar Puli is with the Mechanical Engineering Department of National Institute of Technology, Warangal-506004, Andhra Pradesh, India (e-mail:ravikumar.puli@gmail.com)

K Madhu Murhty is with the Mechanical Engineering Department of National Institute of Technology, Warangal-506004, Andhra Pradesh, India (e-mail:madhumurthyk@gmail.com)

Biofuels have become an alternate to petro diesel in the view of the faster depletion of petro diesel. Understanding the aspects of biodiesel combustion is now possible with the simulation models. Many researchers throughout the world have developed such models. Rao et al [13] has developed a one dimensional, quasi-steady multi zone model from a fuel injection sub model to predict performance and emissions for variables of speed and injection timing. The model successfully predicted the effect of injection timing on the engine and emission parameters. Many other contributions are available on the combustion performance of diesel engine fueled by biofuels [14-16]. However, certain complex models are used nowadays to predict the combustion process more accurately. The literature says that even some zero dimensional models are simple and the efficiency can be compared with the complex models.

II. Present Model For Engine Simulation

An attempt has been made to develop a simple model that can predict the engine combustion performance with different fuels and with selected options of EGR and supercharging. Engine performance, emission parameters obtained from the computer program has been compared to validate the experimental results. The zero dimensional model has been used to find cylinder pressure, heat release rate, brake thermal efficiency and with possible phenomenological models to predict the ignition delay, soot formation , NO formation. Initially the blends of biodiesel diesel blends B10, B20 & B100 and the blends of ethanol diesel E10B, E20B and E30B were tested in the engine with the predetermined test procedure. For engine simulation the design input conditions of an engine speed 1500 RPM and fuel injecting timing of 26^0 BTDC are used, the appropriate other initial conditions were assumed. The fuel properties are shown in table 1, the engine specifications used in the computer program are shown in table 2.

A. Assumptions used in the model

1. Zero-dimensional flow conditions inside the cylinder
2. The gas in the cylinder moves through the equilibrium states
3. No gas leakage through the valves and piston rings so that the mass remains constant
4. Uniform crank speed
5. The cylinder gas is air and it obeys the gas laws
6. The specific heats of the gas mixtures are calculated as a function of temperature

7. Pressure and temperature in the cylinder are uniform and vary with crank angle
8. The details of the computer program start from solving the energy equation, the gas properties calculation, heat release analysis, heat transfer, ignition delay model, calculation of frictional power and emission formation models for finding soot formation, NO formation.

B. Prediction of heat release and gas properties

The equations solved for finding pressure and temperatures a history is shown in equation (1) and (2) which modified form of the energy equation.

$$\frac{dT}{d\theta} = \frac{1}{mc_V}\frac{dQ_c}{d\theta} - \frac{hA_\theta(T_\theta - T_W)}{mC_V} - \frac{RT}{C_V}\frac{1}{V}\frac{dV}{d\theta} \quad (1)$$

$$\frac{dp}{d\theta} = \left(\frac{dQ_n}{d\theta} - \frac{\gamma}{\gamma-1}p\frac{dV}{d\theta}\right)\left(\frac{\gamma-1}{V}\right) \quad (2)$$

The rate of heat release from the cylinder walls has been calculated using equation (3)

$$\frac{dQ_h}{d\theta} = hA_\theta(T_\theta - T_W) \quad (3)$$

In cylinder volume at each crank angle position is calculated using the equation (4)

$$V(\theta) = V_d \times \left[\frac{r}{r-1} - \frac{1-\cos\theta}{2} + \frac{L}{S} - \frac{1}{2}\sqrt{\left(\frac{2L}{S}\right)^2 - \sin^2\theta}\right] \quad (4)$$

The rate of heat release has been estimated from Wiebe's heat release model shown as equation (5)

$$\frac{dQ_c}{d\theta} = a(m+1)\left(\frac{Q_{av}}{\Delta\theta_c}\right)^m \left(\frac{\theta-\theta_i}{\Delta\theta_c}\right)^m exp\left[-a\left(\frac{\theta-\theta_i}{\Delta\theta_c}\right)^{m+1}\right] \quad (5)$$

Gas properties during the compression and expansion have been calculated using isentropic relations shown below

$$P_{\theta+1} = P_\theta\left[\frac{V_\theta}{V_{\theta+1}}\right]^n$$

$$T_{\theta+1} = T_\theta\left[\frac{V_{\theta+1}}{V_\theta}\right]^{n-1}$$

C. Calculation of ignition delay

Ignition delay can be defined as the time interval between the start of fuel injection and the start of combustion. Many researchers have given correlations for predicting ignition delay in which the earliest was Wolfer (1938) [2]. The empirical formula used in the present model is shown in equation which was given by Hardenberg et al. [2]This equation gives the value of ignition delay in terms of values of degrees of crank angle using temperatures (T) in Kelvin and pressure (P) in bar. The equation (6) has been used to predict the ignition delay.

$$\tau_{id} = (0.36 + 0.22\hat{S}_p)exp\left[E_A\left(\frac{1}{RT} - \frac{1}{17190}\right)\left(\frac{21.2}{p-12.4}\right)^{0.63}\right] \quad (6)$$

$$E_A = \frac{B}{CN+25}$$

D .Nitric Oxide Formation

NO formation is modelled using the Zeldovich Mechanism, the amounts of NO formation for each thermodynamic cycle have been predicted using the procedure explained by Turns (2000) [3]. After establishing the temperature and pressure data at each crank angle using zero dimensional model the equilibrium concentrations of the nitrogen and oxygen can be predicted, which is used for better prediction of NO formation. The nitric oxide emissions are computed using equation (7).

$$\frac{d[NO]}{dt} = 2k_{1f}\left(\frac{K_pP^0}{R_uT}\right)^{1/2}[N_2][O_2]^{1/2} \quad (7)$$

$$k_{1f} = 1.82 * 10^{14}e^{\left[\frac{-38370}{T(K)}\right]}$$

$$K_pP^0 = e^{\left(\frac{-\Delta G^0{}_T}{R_uT}\right)}$$

Where $[O]_2$ is the equilibrium oxygen concentration in moles, $[N]_2$ is the equilibrium nitrogen concentration in moles given as

$$[O]_2 = 0.79 * \frac{P}{(Ru*T)}$$

$$[N]_2 = 0.21 * \frac{P}{(Ru*T)}$$

E. Prediction of soot formation

Soot has been predicted using the relation proposed by Patterson et al. (1994) [3] which give the values of soot formation in gm/sec with assumed data. The constants C_{BS} needs to be modified for prediction of soot with the exhaust gas reconciliation process. The following equation (8) has been used for prediction of soot.

$$\frac{dm_{soot}}{dt} = C_{BS} * \Phi * m_f * P^{0.5} * e^{(-E_{sf}/R_aT)} \quad (8)$$

F. Frictional Power Calculations

The equations 9, 10 and 11 were used to calculate the frictional power. It is always desirable to calculate the friction power loss from an engine. The frictional losses not only affect the performance but also increase the size of the coolant system. The empirical relations have been used to predict the friction power losses [4]. The calculation of these friction losses is assumed to be of three components and calculations are made accordingly.

1. Mean effective pressure lost to overcome friction due to gas pressure behind the rings

$$F_{mep1} = 0.42 * (p_a - p_{imf}) * \frac{S}{d^2} * \left(0.0888r + 0.182r^{1.33-0.394\hat{S}_p/100}\right) * 10 \quad (9)$$

2. Mean effective pressure absorbed in friction due to wall tension of rings

$$F_{mep2} = 10 * \frac{0.377 S n_{pr}}{d^2} \quad (10)$$

3. Mean effective pressure absorbed in friction due to piston and rings

$$F_{mep3} = 12.85 * \left(\frac{P_{sl}}{dS} * \frac{100 * \hat{S}_p}{1000}\right) \quad (11)$$

G. Indicated Power and Brake Power calculations

The following equations are used for calculating the indicated power, brake power and brake thermal efficiency

$$IP = \frac{I_{mep} LANK}{60 * 1000}$$

$$BP = IP - FP$$

$$BSFC = \frac{m_f}{BP}$$

$$\eta_{bth} = \frac{BP}{m_f * C_v}$$

H. Combustion duration

Prediction of combustion duration is very important as that of ignition delay. However the correct prediction of combustion duration is difficult for different blend fuels since their C/H ratios and stoichiometric conditions defer from base fuels. The following equation (15) was used to predict the combustion duration for the fuel $C_{10}H_{22}$. And for convenience the combustion duration has been considered as same value for the entire program.

$$\Delta\theta_c = 40 + 5\left(\frac{N}{600} - 1\right) + 166\left(\frac{Ycc}{Y} - 1.1\right)^2 \quad (15)$$

III. General Steps For Approaching The Calculation

The pressure and temperatures at each crank angle step in the cycle are obtained by solving the energy equation; the properties in the combustion period are calculated using Weibe's heat release model. Pressures and temperatures with crank angle are plotted for the entire cycle. Ignition delay period, adiabatic flame temperature, combustion duration, NOx and soot formation are predicted using empirical models. Brake power and brake specific fuel consumption is calculated by using appropriate formulae.

III. Results

P-θ diagram:

The pressure and temperature histories obtained from the program have been analyzed for different fuels. The pressure crank angle diagram can be used to assess the thermodynamic behavior of the engine. It can be observed that there is a modest increase of pressure during the start of compression process to the commencement of fuel injection. The trend is similar for different loads. However, during the combustion period i.e. When the fuel overcomes the ignition delay there is a significant rise in cylinder pressure till the start of the expansion. The peak pressures are observed near TDC position, the higher pressures can be observed during the combustion phase of 334^0 in 384^0, and the higher peaks can be observed at higher loads than that of lower and part loads. The lower peak pressures at lower loads can be attributed to a lower fuel availability for combustion thus having lower heat release rates.

The peak pressures are lowered with ethanol blending with diesel. And supercharging operation resulted in little lowering the maximum combustion pressure, temperatures in comparison to no supercharging case, a very close relation can be observed for diesel with supercharging and no supercharging. The ethanol-diesel blends are inferior to pure diesel in terms of heating value, will have lower instantaneous heat release rates as a consequence the indicated pressure values will be lower for ethanol-diesel blends.

The peak cylinder pressures are low with biodiesel blends in comparison to diesel since the heating value of biodiesel is lower than that of diesel resulting in lower heat release. Poor atomization and slow heat release rate also the reason for lower peak pressure for pure biodiesel. However, these effects will be negligible for small quantity blends (B10) and the results are closer to diesel. The EGR operation resulted in lowering the peak cylinder pressures. The reason for this is charge dilution causes the cylinder to suppress the combustion thus lowering or slow down the heat release, thus lowering the maximum combustion pressure. The indicated pressures versus crank angle graphs are shown in fig.1, fig.2 and fig.3.

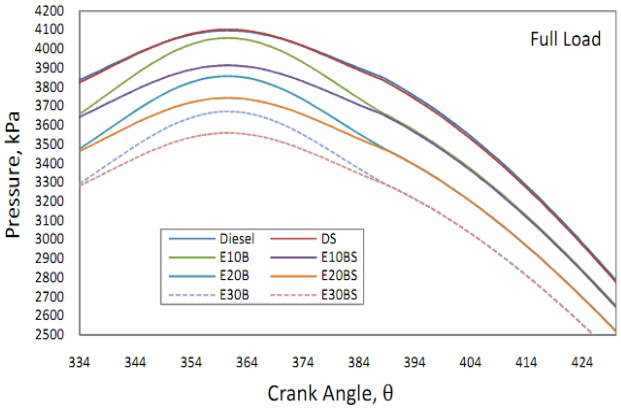

Fig. 1 Pressure versus crank angle for ethanol-diesel blends

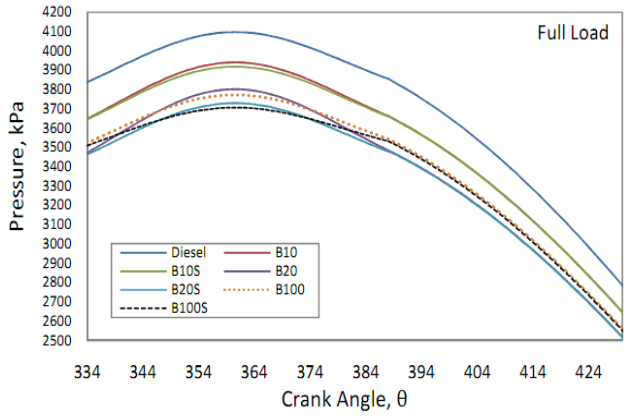

Fig. 2 Pressure versus crank angle for biodiesel-diesel blends

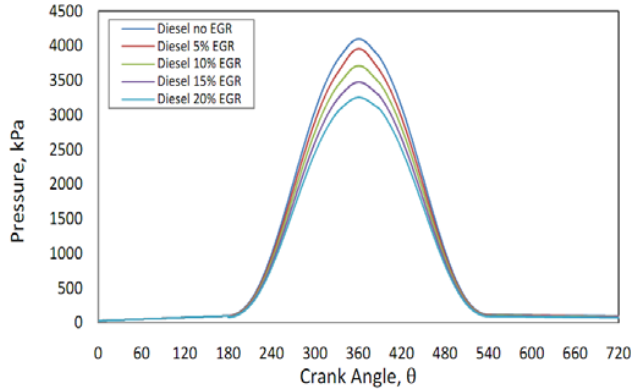

Fig. 3 Pressure versus crank angle for fuel diesel with different EGR rates at full load

T-θ diagram:

Maximum temperature values are decreased with ethanol-diesel and biodiesel-diesel blends due to a reduction in heating values of blends in comparison to neat diesel. The indicated temperature values of no supercharging and supercharging are comparable, however decreased by fewer amounts with supercharging. Since for a constant speed engine the effect of supercharging was observed to reduce fuel consumption.

The EGR affected the combustion by reducing the maximum temperature values, since the NOx formation mainly depends on flame temperature. So, with EGR the conditions for the formation of NOx may be suppressed due to a reduction in local adiabatic flame temperature maximum. This effect is observed for almost all biofuel blends. The T-θ plots for the different fuel blends are shown in fig. 4, fig. 5 and fig. 6.

Ignition Delay:

The ignition delay value for diesel on full load condition is (cetane number 45) obtained as 0.4011 mille seconds, and is little affected by supercharging. However the literature gives the information that supercharging lowers the ignition delay time. The values are increased with EGR like 0.4215, 0.446, 0.4758 and 0.5128 for 5%, 10%, 15% and 20% respectively with fuel

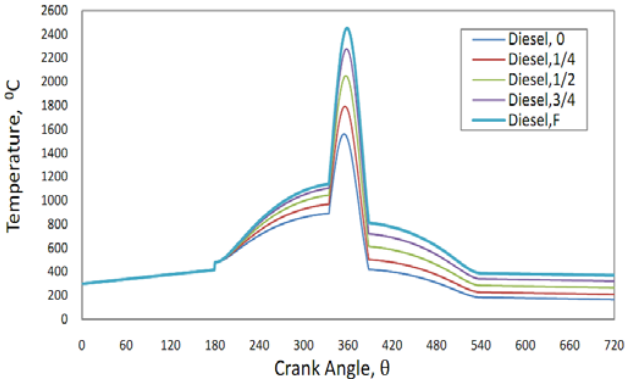

Fig. 4 Temperature versus crank angle for fuel diesel at different loads

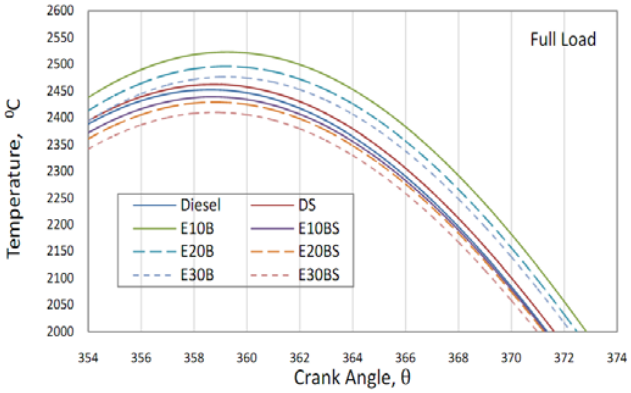

Fig. 5 Temperature versus crank angle for ethanol-diesel blends

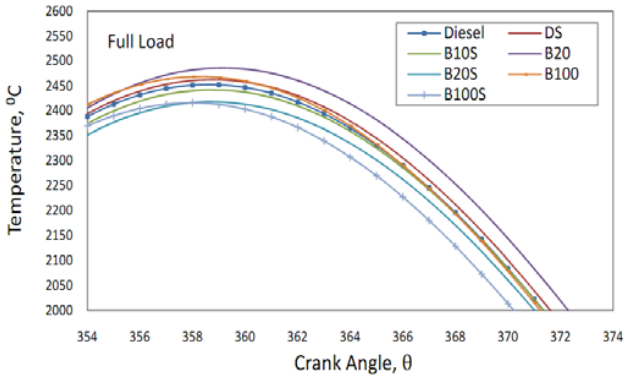

Fig. 6 Temperature versus crank angle for biodiesel-diesel blends

diesel and same trend is observed with different fuels. The ignition delay values for different fuels at full load are 0.4215, 0.446, 0.4758, 0.4215, 0.446, and 0.3491 for E10B, E20B, E30B, B10, B20 and B100 respectively. The low value of ignition delay with B100 was observed since the assumed value of cetane number for biodiesel is 60.

The combustion duration value obtained was 50^0 with fuel diesel and almost assumed same for the entire engine simulation process, since the exact air fuel ratio is needed to estimate the combustion duration. For diesel-biofuel blends this process would be tedious, for simplicity the value of combustion duration was assumed to be 50^0.

Nitric Oxide Emissions:

Nitric oxide emissions with crank angle of the selected engine with variable loads for are shown in fig. 7. Nitric oxide formation calculation is based on Zeldovich mechanism. The NO emissions increase with load on the engine since the maximum combustion temperatures increases with load. At full load E10B showing higher NO emissions among all.

The higher NO emissions in the case of E10B (2509 ppm), B10 (2194 ppm) are due to the presence of the fuel oxygenate in the diesel enhancing the combustion quality causes an increase in maximum combustion temperatures. With E20B, B20 also little high NO emissions are noticed since the presence of high concentration of biofuels caused little high NO emissions compared with the baseline diesel results. With supercharging for the constant speed engine the NO emissions are little reduced when compared with no supercharging, since for constant speed engine there is a reduction of adiabatic flame temperature due to low fuel consumption. The NO emission with crank angle with different fuels is shown in fig. 8.

The NO emissions are little lower for B100 (1312 ppm) in comparison to diesel. However the literature provides information that biodiesel combustion results in higher NOx emissions. The present model calculates the NO formation based on temperature, practically biodiesel combustion results in higher NO emissions due to effects like higher bulk modulus, higher fuel consumptions due to higher densities and the presence of fuel nitrogen in the biodiesel.

The NO emissions are significantly reduced with EGR as shown in the fig.9 with 20% EGR the peak value of NO emissions is nearly 439 ppm whereas with no EGR nearly 1671 ppm. With 5% EGR there has been a rise in NO emissions since unburned hydrocarbons which are sent through EGR may burn giving higher flame temperatures. However, with higher EGR rates there is a reduction in combustion efficiency giving low flame temperatures compared with no EGR.

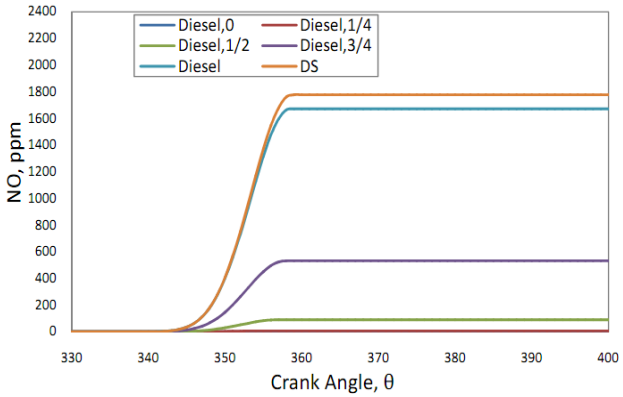

Fig. 7 Nitric oxide emissions with crank angle for fuel diesel with variable loads

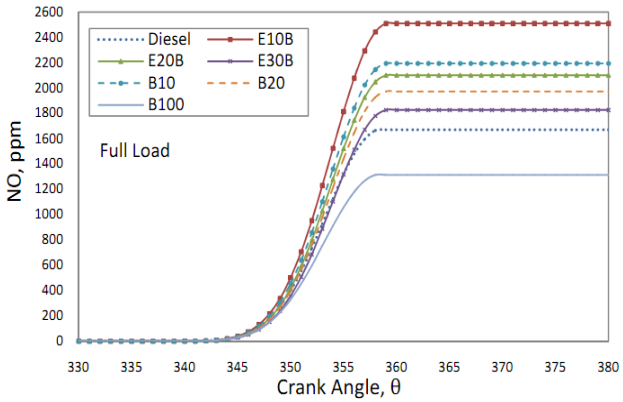

Fig. 8 Nitric oxide emissions versus crank angle with different biofuel blends

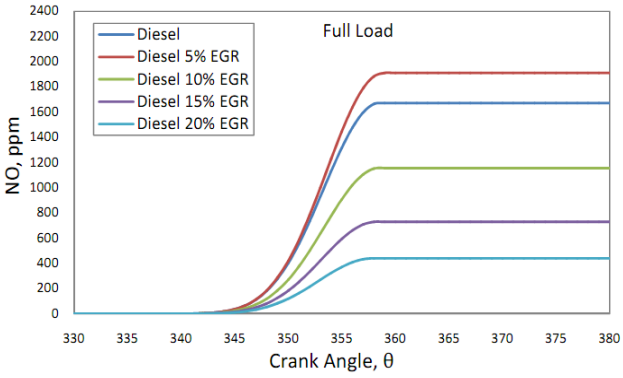

Fig. 9 Nitric oxide emissions versus crank angle with fuel diesel with different EGR rates

Soot Formation:

The soot emissions increase with the load because of higher fuel consumptions and the higher combustion temperatures. Soot emissions with crank angle are shown in fig. 10 at full

load of engine operation. Soot emissions seem to decrease with supercharging due to improved combustion performance with supercharging, and for the present case the reduction in specific fuel consumption with supercharging. The same results can be observed with almost all biofuel blends. When the comparison is made for biofuel blends with diesel, only pure biodiesel showed an observable reduction in soot emissions, and other biofuel-diesel blends showed nearer to diesel except E10B and E20B.

The soot emissions increase enormously with EGR rate due to poor combustion efficiency with the presence of high amounts of residual gases. Soot emissions increased drastically with higher EGR rates (i.e. more than 10%). So it is the indication of the presence of higher PM emissions, so an EGR rate up to 10% can be well suggested keeping in the view of higher soot and PM emissions. The soot emissions with EGR for fuel diesel are presented in fig. 11.

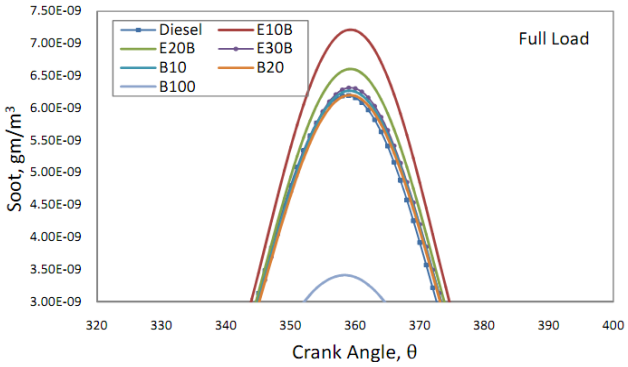

Fig. 10 Emissions of soot versus crank angle with different biofuel diesel blends

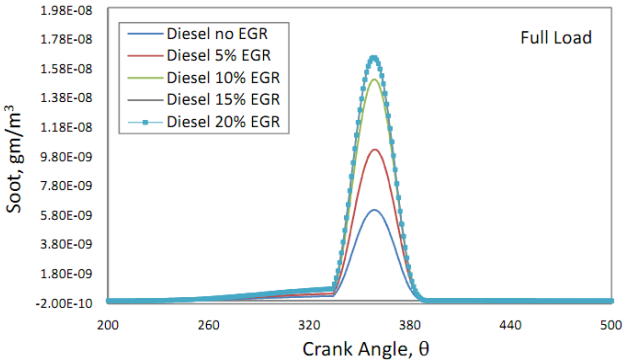

Fig. 11 Emissions of soot with different EGR rates for fuel diesel

IV. Validation of Simulation Results

The simulation results have been validated using experimental results. The comparison of the BSFC values is shown in fig. 12 for fuel diesel; the closeness of the results can indicate the agreement of simulation results with experiment. Similarly the comparison of the values of brake thermal efficiency is presented in fig. 13.

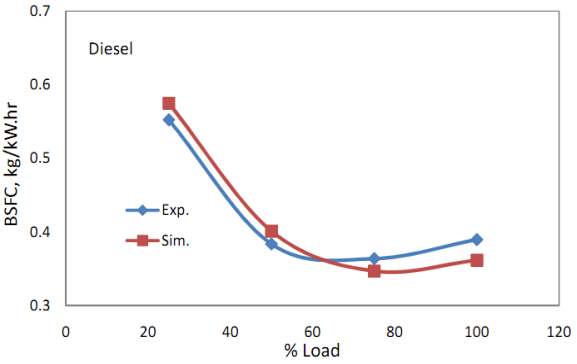

Fig. 12 comparisons of BSFC value with load for fuel diesel

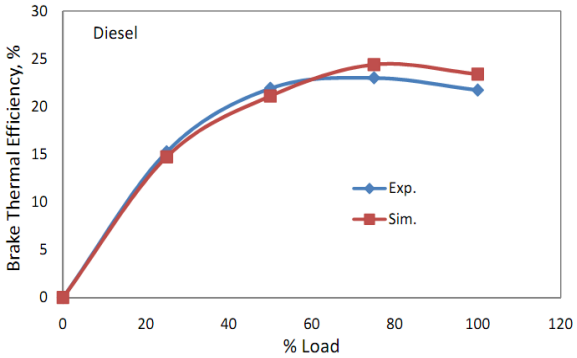

Fig. 13 comparisons of BTE values with load for fuel diesel

V. Conclusions

1. A zero dimensional combustion model simulation has been carried out to predict the single cylinder constant speed diesel engine performance.
2. The engine performance is improved with low quantity blends of biofuels to diesel, this indicated by higher maximum combustion temperatures and pressures when compared with neat diesel.
3. The nitric oxide emissions are reduced with ethanol diesel blends due to low peak cylinder temperatures, and with biodiesel the nitric oxide emissions increased.
4. With EGR the NOx emissions are significantly reduced for all the fuels.
5. The supercharging operation resulted in lowering the peak values of temperature and pressure.
6. The smoke emissions are reduced with biofuel operation in a diesel engine. The smoke formation tendency is aggravated with EGR.
7. The simple model developed has predicted the performance of the given constant speed engine, as an alternate to a complex methodology of multidimensional modeling.
8. The results of the present model are well in agreement with experimental results.

REFERENCES

[1] G.Stiesch, "Modeling engine spray and combustion processes", Springer, 2003.
[2] J.B.Heywood, "Internal Combustion Engines Fundamentals", McGraw Hill Series, New York, 1988.
[3] S.R.Turns, "An introduction to combustion-concepts and applications", McGraw Hill Series in Mechanical Engineering, 2000.
[4] V.Ganesan, "Computer simulation of compression ignition engine processes", University Press, ISBN: 8173712932, 2002.
[5] Lakshmi Narayanan, P.A., Aghav, Y.V, "Modeling Diesel Combustion", Springer, 2009.
[6] C.D.Rakopoulos, K.A.Antonopoulos, D.C.Rakopoulos and D.T.Hountalas, "Multi-zone modeling of combustion and emissions formation in DI diesel engine operating on ethanol–diesel fuel blends", Energy Conversion and Management, 49, No.4, 2008, pp. 625-643.
[7] D.T.Hountalas and A.D.Kouremenos, "Development of a fast and simple simulation model for the fuel injection system of diesel engines", Advances in Engineering Software, 29, No.1, 1999, pp.13-28.
[8] M.Cheikh, B.Abdelhamid, A.Abdelkader and G.Francoise, "Gas-Diesel (dual-fuel) modeling in diesel engine environment", Thermal Science, 40, 2001, pp. 409-424.
[9] J.Ghojel and D.Honnery, "Heat release model for the combustion of diesel water emulsion in DI diesel engines", Applied Thermal Engineering, 25, No.14-15, 2005, pp.2072-2085.
[10] S.Zehra and D.Orhan, "Multi-zone combustion modeling for the prediction of diesel engine cycles and engine performance parameters", Applied Thermal Engineering, 28, 2008, pp.2245-2256.
[11] K.Kannan and M.Udayakumar, "Modeling of nitric oxide formation in single cylinder direct injection diesel engine using diesel-water emulsion", American Journal of Applied Sciences, 6, no.7, 2009, pp. 1313-1320.
[12] T.K.Gogoi and D.C.Baruah, "A cycle simulation model for predicting the performance of a diesel engine fuelled by diesel and biodiesel blends", Energy, vol. 35, Issue 3, 2010, pp.1317-1323.
[13] G.A.P.Rao, "Multi zone modeling of DI diesel engine flow processes", Proceedings of 8th Asia Pacific Conference on Combustion, December, Hyderabad, India, 2010, pp.1321-1327.
[14] C.D.Rakopoulos, D.T.Hountalas and T.C.Zannis, "Theoretical study concerning the effect of oxygenated fuels on DI Diesel engine performance and emissions", SAE Paper No.2004-01-1838.
[15] A.S.Ramadhas, S.Jayaraj and C.Muraleedharan, "Theoretical modeling and experimental studies on biodiesel-fueled engine", Renewable Energy 31, 2006, pp.1813-1826.
[16] C.D.Rakopoulos, K.A.Antonopoulos and D.C.Rakopoulos, "Development and application of multi-zone model for combustion and pollutants formation in direct injection diesel engine running with vegetable oil or its bio-diesel", Energy Conversion and Management 48, 2007, pp.1881-1901.

TABLE I
FUEL PROPERTIES

Property	Diesel	Ethanol	PSME
Density (kg/m$^{3)}$	840	789	874
Kinematic Viscosity (cSt)	2.44	1.52	4.76
Heating Value(kJ/kg)	42,500	29700	39,900
Cloud Point,^{0}C	3	-25	16
Pour Point,^{0}C	-6	-113	19
Flash Point,^{0}C	70	17	145
Cetane number	45	--	60

TABLE II
ENGINE SPECIFICATIONS

Engine Type	Four stroke ,Direct Injection
Number of Cylinders	One
Type of Cooling	Water Cooling
Rated Power	3.7 kW at 1500 rpm
Bore	80 mm
Stroke	110 mm
Compression Ratio	16.5:1
Connecting rod length	230 mm
Volume at TDC	35 CC
Volume at BDC	588 CC
IVO/IVC	4.5^0 bTDC/ 35.5^0 aBDC
EVO/EVC	35.5^0 bBDC/4.5^0 aTDC
Start of fuel injection	26^0 bTDC
Fuel Injection Pressure	18 MPa

ABBREVIATIONS

BSFC	Brake Specific Fuel Consumption [kg/kW.h]
BTDC	Before Top Dead Centre
BTE	Brake Thermal Efficiency [%]
DS	Diesel with Supercharging
E10B	Blend of 10% ethanol,5% ester,85% diesel by volume
E20B	Blend of 20% ethanol,10% ester,70% diesel by volume
E30B	Blend of 30% ethanol,10% ester,60% diesel by volume
E10BS	E10B with supercharging
E20BS	E20B with supercharging
E30BS	E30B with supercharging